

In Vivo Polarization of IFN- γ at Kupfer and Non-Kupfer Immunological Synapses during the Clearance of Virally Infected Brain Cells^{1,2}

Carlos Barcia,*[†] Kolja Wawrowsky,*[†] Robert J. Barrett,*[†] Chunyan Liu,*[†] Maria G. Castro,*[†] and Pedro R. Lowenstein^{3*†}

Kupfer-type immunological synapses are thought to mediate intercellular communication between antiviral T cells and virally infected target Ag-presenting brain cells in vivo during an antiviral brain immune response. This hypothesis predicts that formation of Kupfer-type immunological synapses is necessary for polarized distribution of effector molecules, and their directed secretion toward the target cells. However, no studies have been published testing the hypothesis that cytokines can only form polarized clusters at Kupfer-type immunological synapses. Here, we show that IFN- γ and granzyme-B cluster in a polarized fashion at contacts between T cells and infected astrocytes in vivo. In some cases these clusters were found in Kupfer-type immunological synapses between T cells and infected astrocytes, but we also detected polarized IFN- γ at synaptic immunological contacts which did not form Kupfer-type immunological synaptic junctions, i.e., in the absence of polarization of TCR or LFA-1. This indicates that TCR signaling, which leads to the production, polarization, and eventual directed secretion of effector molecules such as IFN- γ , occurs following the formation of both Kupfer-type and non-Kupfer type immunological synaptic junctions between T cells and virally infected target astrocytes in vivo. *The Journal of Immunology*, 2008, 180: 1344–1352.

We have recently shown that effector CD8⁺ T cells establish characteristic Kupfer-type immunological synapses in vivo with adenovirally infected brain astrocytes during their clearance from the brain (1). Kupfer-type immunological synapses are characterized by the polarized distribution of LFA-1 and TCR to form the supramolecular activation clusters (SMAC)⁴ at the T cell membrane facing the synaptic in-

terface. LFA-1 becomes concentrated to an outer ring called the peripheral-SMAC (p-SMAC), whereas TCR concentrates in the inner region, the central-SMAC (c-SMAC) (1–3). The microtubule organizer center (MTOC) and Golgi apparatus of T cells also reorient toward the immunological synapse (4, 5). This reorganization of T cell structure and the formation of immunological synapses is thought to direct secretion of effector molecules, such that IFN- γ and granzyme B are secreted through the immunological synapse, whereas TNF- α is secreted outside of the immunological synapse (6). However, whether directed targeting of T cell effector molecules can occur in vivo, and whether this depends on the formation of a Kupfer-type immunological synapse in the context of an antiviral immune response in vivo remains unknown.

Immunological synapses are thought to be the microanatomical structure underlying intercellular communication in the immune system (1, 7, 8). They form between naive T cells and dendritic cells during T cell priming, and between CD4⁺ and CD8⁺ T cells and target cells during the effector stage of the immune response. However, most work in this field so far has used in vitro models to study the formation and function of immunological synapses (2, 6, 7, 9–19). During the formation of immunological synapses T cells become polarized and oriented toward the interface with the target cells (6, 9); at the interface T cells form a central and peripheral supramolecular activation cluster (c-SMAC and p-SMAC) (2, 3, 7, 10), and redistribute their entire cytoplasm and organelles toward the synaptic interface.

There has been some controversy as to whether the term immunological synapse should only be applied to Kupfer-type junctions displaying the c-SMAC and p-SMAC, or whether the term should be applied more generally to the interface formed between immune cells, or between immune cells and their target cells (11–14). Furthermore, T cell activation and effector functions have been proposed to proceed in the presence or absence of the morphological differentiation of the SMACs characteristic features of the Kupfer-type synapses (8, 11–13, 32). Thus, it has been recently proposed that the

* Board of Governors' Gene Therapeutics Research Institute, Cedars-Sinai Medical Center, Los Angeles, CA 90048; and Department of Medicine, and Department of Molecular and Medical Pharmacology, [†]David Geffen School of Medicine, University of California Los Angeles, Los Angeles, CA 90095

Received for publication September 25, 2007. Accepted for publication November 12, 2007.

The costs of publication of this article were defrayed in part by the payment of page charges. This article must therefore be hereby marked *advertisement* in accordance with 18 U.S.C. Section 1734 solely to indicate this fact.

¹ This article is dedicated to the memory of Enrique C. Lowenstein (22 December 1914–18 April 2007). "Les vrais paradis sont les paradis qu'on a perdus." Marcel Proust

² This work is supported by National Institutes of Health/National Institute of Neurological Disorders and Stroke Grant 1R01 NS44556.01, Minority Supplement NS445561.01, 1R21-NS054143.01, 1U01 NS052465.01, 1R03 TW006273-01 (to M.G.C.), National Institutes of Health/National Institute of Neurological Disorders and Stroke Grants 1R01 NS 054193.01; R01 NS 42893.01, U54 NS045309-01 and 1R21 NS047298-01 (to P.R.L.), The Bram and Elaine Goldsmith and the Medallions Group Endowed Chairs in Gene Therapeutics (to P.R.L. and M.G.C., respectively), The Linda Tallen and David Paul Kane Foundation Annual Fellowship, and the Board of Governors at Cedars-Sinai Medical Center.

C.B. performed the research, analyzed the data, and contributed to writing the paper, K.W. provided the 3-D reconstruction software and analyzed the data, R.B. analyzed the data and contributed to writing the paper, C.L. prepared the viral vectors, and M.G.C. and P.R.L. designed the research, analyzed the data, and wrote the paper.

³ Address correspondence and reprint requests to Dr. Pedro R. Lowenstein, Board of Governors' Gene Therapeutics Research Institute, Cedars-Sinai Medical Center, 8700 Beverly Boulevard, Room 5090, Los Angeles, CA 90048. E-mail address: lowensteinp@cshs.org

⁴ Abbreviations used in this paper: SMAC, supramolecular activation clusters; c-SMAC, central supramolecular cluster; p-SMAC, peripheral supramolecular cluster; DAPI, 4',6-diamidino-2-phenylindole.

term immunological synapse be used in a more general way to describe all interfaces between immune cells, and the term Kupfer-type synapse be used for those structures displaying SMACs (14). Therefore, as recently proposed, we decided to reserve the term 'Kupfer-type' immunological synapse to designate immune interfaces establishing SMACs, and use 'non-Kupfer type' contact to refer to all other junctions formed by T cells and their target cells in the brain (14).

Previously, we have been able to show that *bona fide* Kupfer-type immunological synapses exist in vivo in the brain during the clearance of infected astrocytes by CD8⁺ T cells. During the anti-adenoviral immune response in rats CD8⁺ T cells peak in the brain fourteen days after anti-adenoviral immunization, while CD4⁺ T cells peak at thirty days postimmunization. Furthermore, only CD8⁺ T cells infiltrate the brain parenchyma, while CD4⁺ T cells remain within the perivascular compartment (1). CD8⁺ CTLs infiltrate the brain parenchyma, interact with target astrocytes, with which they establish Kupfer-type intercellular junctions. As a consequence of cognate Ag recognition on target cells' MHC, the TCR triggers T cell activation, leading to the phosphorylation of Lck and ZAP-70 and their congregation at synaptic junctions (1, 15–19). T cell activation is known to lead to the production and secretion of effector molecules IFN- γ , perforin and granzyme-B (6, 20–22). The relationship between the structural reorganization of T cells and its functional outcomes, and their dependence on the formation of Kupfer-type immunological synapses is currently under much investigation (7).

To explore the interaction between T cells and target cells in vivo we have used a well known model in rats in which adenoviral infected astrocytes in the brain are cleared by T cells (1). In this model a recombinant replication-defective adenovirus is used to infect mostly brain astrocytes. Infected astrocytes can be recognized because they express a gene, herpes-simplex virus thymidine kinase (HSV1-TK), only expressed by the adenovirus. A systemic anti-adenovirus immune response is then stimulated through the immunization with adenovirus; this results in the infiltration of the brain with antiviral T cells, and the eventual clearing of infected brain astrocytes (1). We have previously demonstrated that T cells specifically activated against adenovirus form Kupfer-type effector immunological synapses with adenovirally infected astrocytes (1). This model has allowed us to study in vivo immunological synapses forming SMAC and the interactions between CTLs and target astrocytes that we believe eventually lead to the clearance of infected astrocytes (1).

Previous work in vitro has questioned whether Kupfer-type synapses were necessary for CTL killing (12, 23, 24); i.e., whether the formation of a morphological identifiable immunological synapse is necessary for effector T cell function (9, 32). Herein we tested the hypothesis that effector molecules such as IFN- γ and granzyme-B are polarized in T cells that form Kupfer-type junctions with target astrocytes. In the present work we demonstrate that both IFN- γ and granzyme-B become polarized and clustered at immunological synapses in vivo between CD8⁺ T cells and virally infected astrocytes. Intriguingly, IFN- γ was also polarized at intercellular junctions between T cells and infected astrocytes that formed non-Kupfer immunological synaptic contacts, i.e., in the absence of SMAC formation by LFA-1 and TCR. Our data suggest that full activation, and potential directed secretion of effector molecules from T cells toward target cells, may occur at either Kupfer or non-Kupfer immunological synaptic junctions.

Materials and Methods

Adenoviral vectors

Adenoviruses used in this study were first-generation E1/E3-deleted recombinant adenovirus vectors based on adenovirus type 5. RAAdTK (expressing herpes simplex virus type I thymidine kinase, HSV1-TK) and

RAAdHPRT (expressing hypoxanthine-guanine phosphoribosyl-transferase), contain the hCMV promoter; their construction has been described in detail elsewhere (25).

Animals, surgical procedures, viruses

Adult male Sprague-Dawley rats (250g body weight) (Charles River) were used according to CSMC's IACUC-approved protocols. A total of 35 animals were injected unilaterally in the left striatum with 1×10^7 i.u. of RAAdTK in a volume of 1 μ l at day 0 to infect astrocytes with adenoviral vector. One month later, rats were anesthetized briefly and injected intradermally with 100 μ l of either sterile saline ($n = 10$, [not-immunized]), or 5×10^8 infectious units of RAAdHPRT ($n = 25$, [immunized]). Animals were sacrificed 14 days after immunization which is the time point of maximum infiltration of CD8 T cells in the brain parenchyma and the maximum peak of interaction between virally infected cells and T cells (1). Animals were anesthetized by overdose and transcardially perfused-fixed with 200–500 ml of oxygenated Tyrode solution. Immediately afterward, animals were perfused with 4% paraformaldehyde to fix the brain. Brains were sectioned on a vibratome (Leica Instruments, Exton, PA) at 50 μ m section thickness.

Immunocytochemical procedures and confocal analysis

Coronal brain sections (50 μ m) were cut serially through the striatum, and immunofluorescence detection was performed as described (1, 26), using the following primary Abs recognizing: TK (1:10,000; rabbit polyclonal, custom made by our laboratory) (1, 25), TK (1:1,000; chicken polyclonal, custom made by AvesLabs Inc.) (27), LFA-1 (1:500; mouse monoclonal, IgG2a, BD PharMingen, clone WT.1), TCR (1:100; mouse monoclonal anti-TCR $\alpha\beta$, IgG1, BD PharMingen, clone R73), IFN- γ (1:100; goat polyclonal anti-rat IFN- γ , R&D systems), granzyme-B (prediluted; rabbit polyclonal Abcam), and macrophages/activated microglia (mouse anti-ED1; 1:1,000, Serotec, clone ED1).

Immunocytochemical detection methods were optimized during preliminary experiments to achieve full and homogenous Ab penetration throughout the total thickness of vibratome sections. Adjacent 50 μ m thick sections of each brain were pretreated with citrate buffer for 30 min at 65°C to increase Ag retrieval and penetration of the Abs into the tissues. Specifically for anti IFN- γ Ab, sections were pretreated with trypsin 0.05% for 10 min at 37°C and for granzyme-B Ab sections were boiled in citrate buffer during 10 min. Sections were blocked with 1% Triton X-100 for 5 min and 10% normal horse serum in 0.1 M PBS, pH 7.4, for 60 min. Sections were incubated at room temperature for 48h with primary Abs. For multiple labeling immunocytochemistry the incubation with primary Ab was followed by 4 h of incubation with the appropriate secondary Abs, Alexa 488, Alexa 546, Alexa 594 and/or Alexa 647 (1:1,000; Molecular Probes). After washing, sections were incubated with DAPI solution for 30 min. Sections were washed, mounted, and examined with fluorescence microscopy (Zeiss), and analyzed with the confocal microscope (Leica).

Brain sections were examined using a Leica DMIRE2 confocal microscope (Leica Microsystems, Exton, PA) with 63 \times oil objective and Leica Confocal Software (Leica Microsystems Heidelberg 19 GmbH). A series range for each section was determined by setting an upper and lower threshold using the Z/Y position for spatial image series setting, and confocal microscope settings were established and maintained by Leica and local technicians for optimal resolution. Contacts were defined as areas where colocalization of both markers occurs between two cells in at least two 0.5 μ m thick optical sections. Contacts can also be illustrated as they appear throughout the stack of sections as a simple 0.5 μ m layer or as a transparency of all layers merged together.

Three dimensional reconstructions to allow rotation of the images were rendered with α blending software (custom made by KW). Brain sections from 35 animals were studied; >200 immunological synapses at various stages of development were recorded and analyzed in detail.

Quantifications

In total the data described reflect the analysis of >200 immunological synapses. In detail, the numbers examined are given in each figure legend. Relative fluorescence intensity along different structures and plane of the immunological synaptic interface was measured with Leica confocal software, and is illustrated in the figures with corresponding arrows traversing the measured optical planes. Quantification of the distribution of IFN- γ expression in T cells was made throughout the T cells' cytoplasm. Twenty one IFN- γ expressing synapses were quantified. Results were expressed as absolute number of positive cells in the anatomical regions analyzed. Data were expressed as the mean \pm SEM.

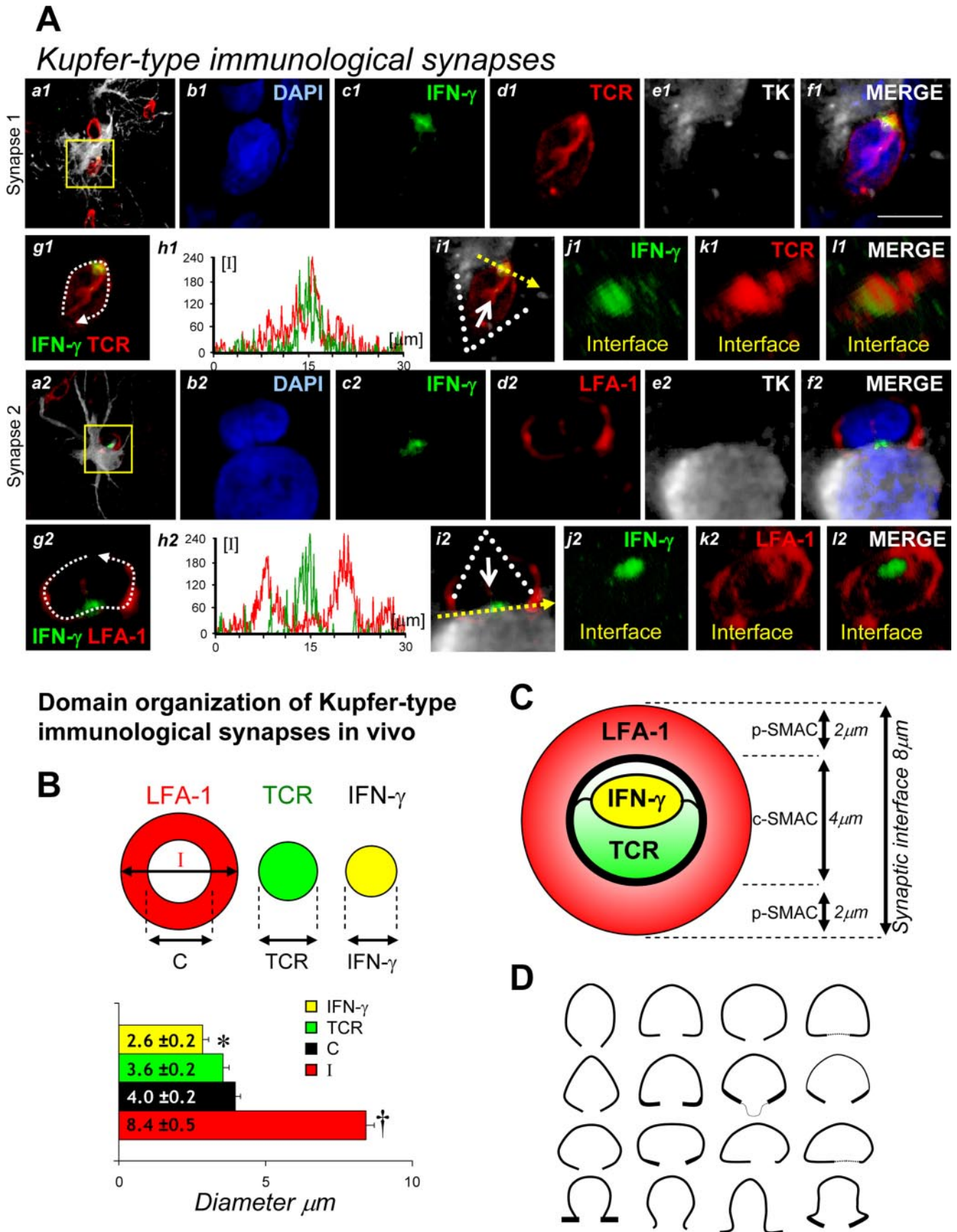


FIGURE 1. T cells establishing Kupfer-type immunological synapses display IFN- γ that is polarized toward virally infected cells. **A**, Two Kupfer-type immunological synapses, with the characteristic central distribution of TCR (defining the c-SMAC), and the peripheral distribution of LFA-1 (defining the p-SMAC), and which express IFN- γ are illustrated in detail. Immunological synapses were stained for IFN- γ (green) and TCR (red) (synapse 1, *top two rows*); or IFN- γ (green) and LFA-1 (red) (synapse 2, *bottom two rows*) combined with HSV1-TK (white, a marker protein expressed by adenovirally infected cells), and nuclear staining (DAPI, blue). *a1*, A three dimensional composite of the stack of confocal images at low power throughout the tissue

Statistical analysis

Data were expressed as mean \pm SEM and evaluated by one-way ANOVA (followed by Tukey's test) or Student's *t* test. Differences were considered significant if $p < 0.05$.

Results

IFN- γ is polarized in T cells forming Kupfer-type immunological synapses; supramolecular activation clusters are stable structures at Kupfer-type immunological synapses

To determine whether T cell effector molecules would be targeted in a polarized manner toward the interface of immunological synapses we studied the distribution of IFN- γ in T cells establishing immunological synaptic contacts with infected brain astrocytes. A total of 21 immunological synapses formed by T cells and expressing IFN- γ could be reconstructed, and were examined in detail. IFN- γ was polarized to the interface of T cells establishing close contacts with adenovirally infected astrocytes. IFN- γ immunoreactivity formed a cluster at the contact interface. Polarized IFN- γ immunoreactive clusters were detected in T cells establishing the typical polarized distribution of TCR in the c-SMAC, and LFA-1 throughout the p-SMAC, characteristic of the Kupfer-type immunological synapses (synapse 1 and 2 in Fig. 1A).

The organization of LFA-1 immunoreactive p-SMAC and TCR immunoreactive c-SMAC, and their relationship to infected astrocytes, were analyzed quantitatively on >200 immunological synapses. IFN- γ -immunoreactive clusters were analyzed in 21 immunological synapses that were immunoreactive for either IFN- γ and LFA-1 or IFN- γ and TCR, and were tightly apposed to infected astrocytes. The extent of the external boundary of the LFA-1 ring was used to determine the diameter of the interface (I in Fig. 1B, C). The region within the internal ring of LFA-1 (which is devoid of LFA-1) was considered the c-SMAC (Fig. 1B, C). Quantitative analysis indicated that the Kupfer-type immunological synaptic interface *in vivo* extends over $8.4 \pm 0.5 \mu\text{m}$ diameter (Fig. 1B). The p-SMAC, labeled by LFA-1, occupies a ring of approximately $2 \mu\text{m}$ diameter, delineating the c-SMAC as a region of $4 \pm 0.2 \mu\text{m}$ diameter. Within the c-SMAC, the area occupied by TCR and IFN- γ was 3.6 ± 0.2 and 2.6 ± 0.2 respectively (Fig. 1B). A detailed analysis of these interfaces revealed that IFN- γ localizes to an intracellular location that overlaps with the

Kupfer-type immunological synapse (still frames from Supplementary movie 1)

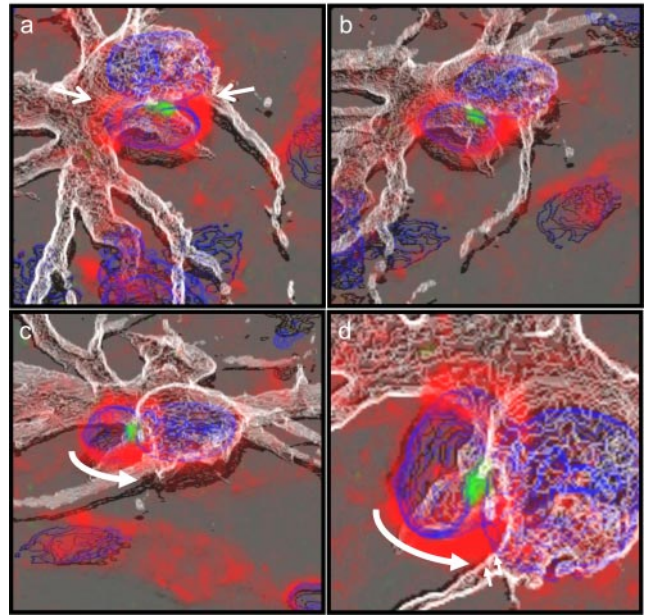
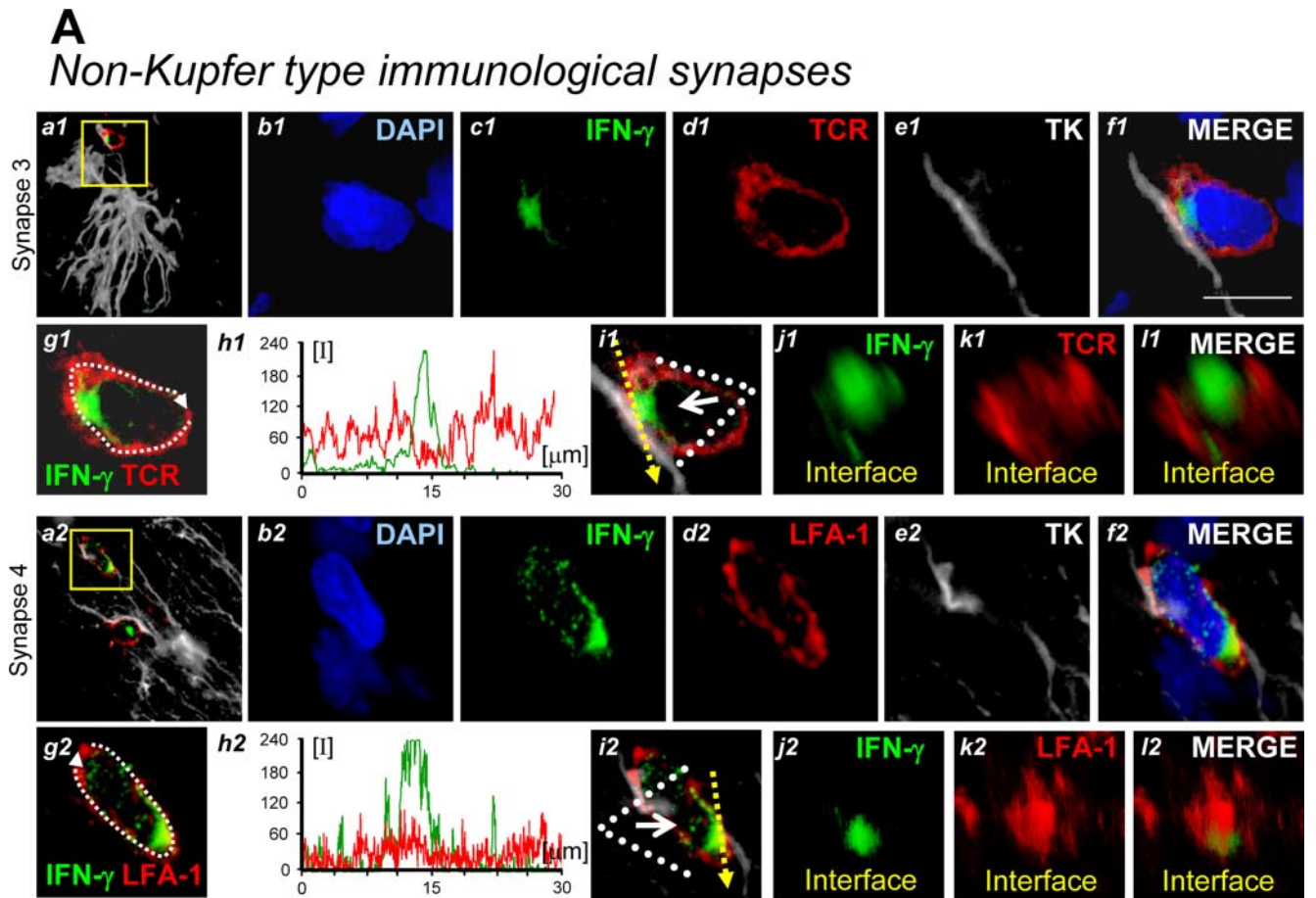


FIGURE 2. Still frames from a movie of a 3-D reconstruction of a Kupfer-type immunological synapse. This figure highlights four individual frames from Supplementary Movie 1 to clarify the formation of this Kupfer-type immunological synapse being formed onto the cell body of an infected brain cell (HSV1-TK, white). Notice the polarized clustering of IFN- γ (green) closely apposed to the cell body of an infected cell (*a–d*) and the polarized distribution of LFA-1 (red), forming the characteristic Kupfer-type p-SMAC. The straight arrows in (*a*) indicate the boundaries of the synaptic contact established onto the cell body (*b*); the curved arrows in (*c*, *d*) indicate the accumulation of LFA-1 at the p-SMAC.

c-SMAC (identified by TCR), and is central to the p-SMAC LFA-1 ring. These measurements displayed a small statistical error, regardless of the different LFA-1 ring shapes (Fig. 1D), indicating the stability of the c-SMAC structure. Fig. 2 are still frames from Supplementary Movie 2 showing the 3-D reconstruction of Synapse 3 depicted in Fig. 1A.

section illustrating T cells (TCR, red) in close apposition with the cell body of a virally infected cell (HSV1-TK, white). *b1–e1*, High power images of the area outlined in the yellow box in *a1* showing nuclei (blue, DAPI), IFN- γ (green), TCR (red), and the cell body of a virally infected cell (HSV1-TK, white). *f1*, Merged images of DAPI (*b1*), IFN- γ (*c1*), TCR (*d1*), and the infected cell (*e1*) illustrating the polarized distribution of IFN- γ (green) at the immunological synapse with the virally infected cell body and colocalization with the accumulation of TCR in the c-SMAC. *h1*, Fluorescence intensity graph of IFN- γ (green) and TCR (red) along the cell outline (white line, *g1*) demonstrating the colocalization of highest levels of intensity of IFN- γ and TCR along the c-SMAC of the immunological synapse. *i1–l1*, 3-D images were reconstructed along the interface (yellow line) and viewed en face (from the direction of the white arrow) to reveal polarized distribution of IFN- γ (*j1*, green) and c-SMAC (*k1*, TCR, red). *l1*, Merged 3-D reconstructed images showing the localization of IFN- γ to the c-SMAC outlined by TCR. *a2*, A three dimensional composite of the stack of confocal images at low power throughout the tissue section illustrating T cells (LFA-1, red) in close apposition with the cell body of a virally infected cell (HSV1-TK, white). *b2–e2*, High power images of the area outlined in the yellow box (*a2*) showing nuclei (blue, DAPI), IFN- γ (green), LFA-1 (red), and a virally infected cell (HSV1-TK, white). *f2*, Merged image of DAPI (*b2*), IFN- γ (*c2*), LFA-1 (*d2*), and the infected cell (*e2*) illustrating the polarized distribution of IFN- γ (green) at the center of the immunological synapse (c-SMAC) with the virally infected cell body; LFA-1 outlines the p-SMAC. *h2*, Fluorescence intensity graph of IFN- γ (green) and LFA-1 (red) along the cell outline (white line, *g2*) demonstrating the highest levels of intensity of LFA-1 were along the peripheral compartment of the immunological synapse, i.e., p-SMAC, surrounding the IFN- γ located within the c-SMAC. *i2–l2*, 3-D images were reconstructed along the interface (yellow line) and viewed en face (from the direction of the white arrow) to reveal the polarized distribution of IFN- γ (*j2*, green) and p-SMAC (*k2*, LFA-1, red). *l2*, Merged 3-D reconstructed images showing the localization of IFN- γ central to the p-SMAC outlined by LFA-1. Scale bar (*f1*) = $10 \mu\text{m}$. *B* shows a schematic of the method to quantitate the diameter of the various constituents of the Kupfer-type immunological synapses. The diameter of the interface (I) at mature immunological synapses was defined by the external limit of the LFA-1 ring (p-SMAC), the diameter of the c-SMAC was defined by the internal boundary of LFA-1, the diameter of TCR cluster was determined by TCR expression, and the diameter of the area occupied by IFN- γ immunoreactivity was also measured. *, $p < 0.05$ with respect to C, indicating that the area occupied by IFN- γ is smaller than the c-SMAC; †, $p < 0.05$ with respect to IFN- γ , TCR and C, indicating that c-SMAC, and the immunoreactivity of TCR and IFN- γ were smaller than the p-SMAC. No statistical difference was found between TCR and c-SMAC quantitation. *C* shows that the average diameter of the synaptic interface (I) was $\sim 8 \mu\text{m}$, the diameter of c-SMAC was $\sim 4 \mu\text{m}$. The IFN- γ cluster displayed a smaller diameter ($\sim 2.6 \mu\text{m}$) significantly different from the c-SMAC. *D* illustrates the various morphologies adopted by the p-SMAC, defined by LFA-1 immunoreactivity. Measurements of LFA-1 (used to calculate pSMAC and c-SMAC) were taken using the confocal software, and are based on the quantification of 39 synapses; the quantification of the IFN- γ and TCR in Kupfer-type synapses is from 7 immunological synapses.



Domain organization of non-Kupfer type immunological synapses in vivo

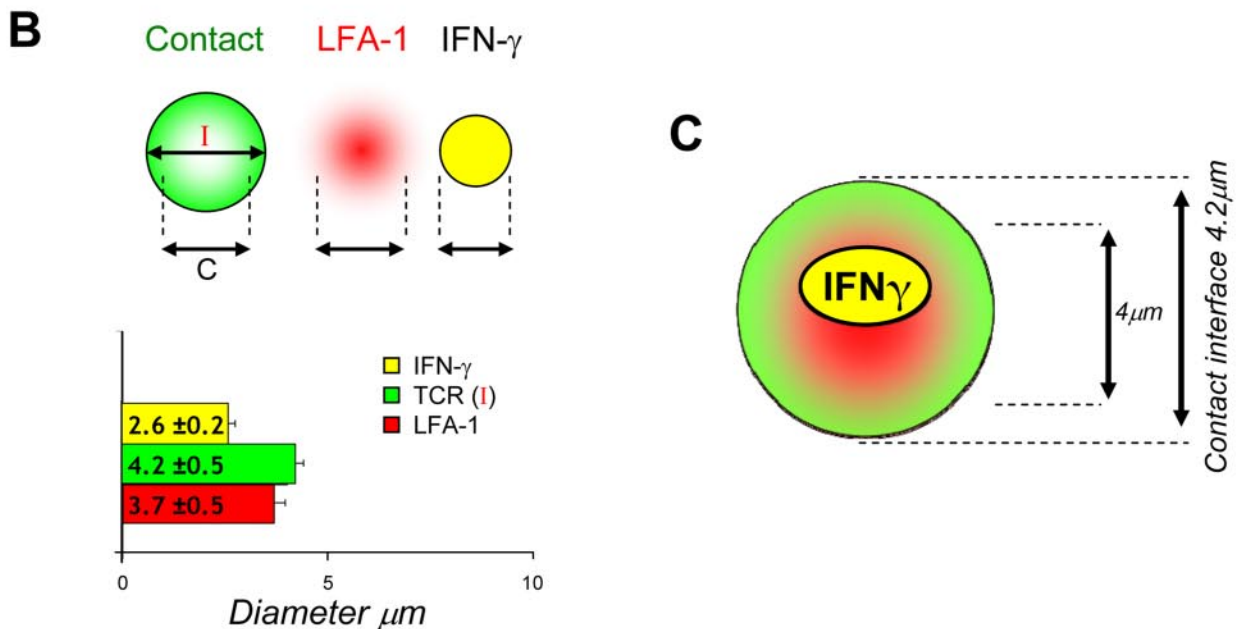


FIGURE 3. T cells establishing non Kupfer-type immunological synaptic contacts display IFN- γ that is polarized toward virally infected cells. (A) Two non-Kupfer-type immunological synaptic contacts, defined by the absence of the characteristic distribution of TCR and LFA-1 to the c-SMAC or p-SMAC in Kupfer-type synapses, respectively, and which express IFN- γ are illustrated in detail. Immunological synaptic contacts were stained for IFN- γ (green) and TCR (red) (Synapse 3, top two rows); or IFN- γ (green) and LFA-1 (red) (Synapse 4, bottom two rows) combined with HSV1-TK (white, a marker protein expressed by adenovirally infected cells), and nuclear staining (DAPI, blue). *a1*, A three dimensional composite of the stack of confocal images at low power throughout the tissue section illustrating T cells (TCR, red) in close apposition with a process of a virally infected cell (HSV1-TK, white). *b1-f1*, High power images of the area outlined in the yellow box (*a1*) showing nuclei (blue, DAPI), IFN- γ (green), TCR (red), and a virally infected cell (HSV1-TK, white). *f1*,

IFN- γ is also polarized in T cells forming non-Kupfer-type immunological synaptic contacts

Quantitative analysis of the relative fluorescence and three dimensional reconstructions demonstrate the formation of central clusters of IFN- γ directly at the intercellular interfaces of immunological synaptic contacts between T cells and infected astrocytes (synapse 3 and 4 in Fig. 3A). TCR occupied an area of $4.2 \pm 0.5 \mu\text{m}$, LFA-1, $3.7 \pm 0.5 \mu\text{m}$, and IFN- γ $2.6 \pm 0.2 \mu\text{m}$ (Fig. 3B, C). Thus, IFN- γ clusters are present in both types of synaptic junctions. The presence or absence of a c-SMAC or p-SMAC does not seem to influence formation of polarized clusters of IFN- γ . Importantly, the size of the area occupied by IFN- γ immunoreactivity is significantly larger in non-Kupfer type synapses compared with those exhibiting the Kupfer-type (Fig. 5B). Fig. 4 are still frames from Supplementary Movie 2 showing the 3-D reconstruction of Synapse 3 depicted in Fig. 3A.

Immunological synapses localize preferentially to the cell bodies of infected Ag presenting astrocytes

Astrocytes are multipolar cells. In principle, immunological synapses could be formed onto either the cell bodies and/or the cellular processes of infected astrocytes. A qualitative analysis indicated that we could detect Kupfer-type immunological synapses on both cell bodies and astrocyte processes. To establish whether there was any preference in the anatomical positioning of immunological synapses, we quantified the location of 143 immunological synapses between CTLs and infected astrocytes (Fig. 5A). Immunological synapses were defined as close appositions between T cells and infected astrocytes, in which membrane contacts could be visualized in two to three adjacent $0.5\text{--}1 \mu\text{m}$ optical confocal sections. Kupfer-type immunological synapses were characterized by TCR-immunoreactivity focused onto a polarized c-SMAC, or LFA-1 immunoreactivity distributed in a typical p-SMAC ring.

A detailed quantitative analysis (illustrated in Fig. 5) of the distribution and characteristics of all immunological synapses indicated that the majority (approx. 70%) were established with the cell bodies of infected astrocytes. Of these, 64% were Kupfer-type synaptic contacts, and 36% formed non-Kupfer type junctions. Of the total amount of synaptic contacts formed onto astrocyte processes (31% of total), half were Kupfer-type. Thus, the majority of immunological synapses were established onto the cell body of infected astrocytes, and 64% of those were Kupfer-type, while those established onto astrocyte processes only 50% are Kupfer-type. Overall, 60% of the total number of immunological synapses are of the Kupfer-type.

**Non-Kupfer-type immunological synapse
(still frames from Supplementary movie 2)**

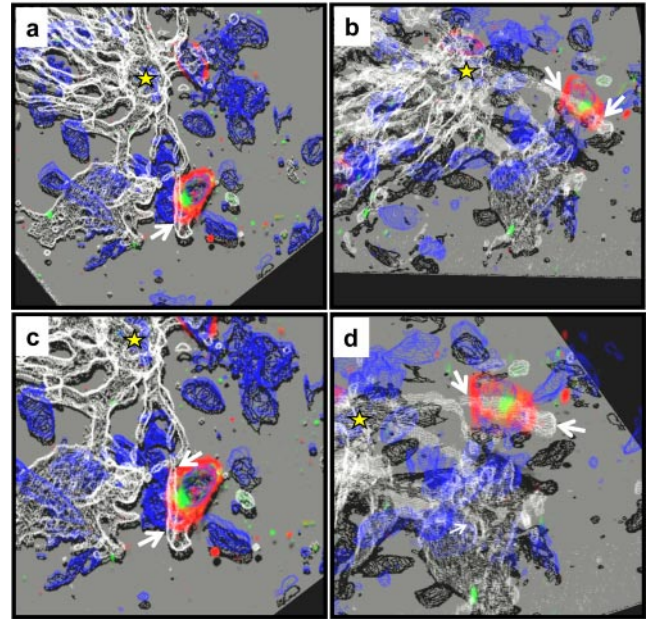


FIGURE 4. Still frames from a movie of a 3-D reconstruction of a non-Kupfer-type immunological synapse. This figure highlights four individual frames from Supplementary movie 2 to clarify the formation of this non-Kupfer type immunological synapse being formed onto a distal process of an infected astrocyte. The yellow star indicates the cell body of the virally infected astrocyte (HSV1-TK, white). Notice the polarized clustering of IFN- γ (green) closely apposed to a process of an infected cell, and the homogeneous distribution of TCR (red), characteristic of non-Kupfer-type immunological synaptic contacts. The arrows indicate the cell process in close contact of the immunological synapse.

Surprisingly, an analysis of the synapses displaying IFN- γ clusters showed an almost inverse distribution (Fig. 5A). Here a majority (71%) of IFN- γ containing synapses were established onto astrocyte processes, and the majority of these were of the non-Kupfer type.

Thus, the population of IFN- γ immunoreactive immunological synapses appears to be a subtype (either morphological, or most likely functional) of all immunological synapses, with most being established onto the astrocyte processes, and most being of the non-Kupfer type. Also, an analysis of the total amount of T cells within the brain, indicated that only approximately 19% expressed

Merged images of DAPI (*b1*), IFN- γ (*c1*), TCR (*d1*), and the infected cell (*d1*) illustrating the polarized distribution of IFN- γ (green) at the immunological synaptic contact with the virally infected cell process. *h1*, Fluorescence intensity graph of IFN- γ (green) and TCR (red) along the cell outline (white line, *g1*); notice that the highest levels of IFN- γ are located centrally. *i1*, 3-D images were reconstructed along the interface (yellow line) and viewed en face (from the direction of the white arrow) to reveal polarized distribution of IFN- γ (*j1*, green) and peripheral distribution of TCR (*k1*, red). *l1*, Merged 3-D reconstructed image showing the localization of IFN- γ at the immunological synaptic contact. *a2*, A three dimensional composite of the stack of confocal images at low power throughout the tissue section illustrating T cells (LFA-1, red) in close apposition with a process of a virally infected cell (HSV1-TK, white). *b2–f2*, High power confocal images of the area outlined in the yellow box (*a2*) showing nuclei (blue, DAPI), IFN- γ (green), LFA-1 (red), and a virally infected cell (HSV1-TK, white). *j2*, Merged images of DAPI (*b2*), IFN- γ (*c2*), LFA-1 (*d2*), and the infected cell (*e2*) illustrating the polarized distribution of IFN- γ (green) at the immunological synaptic contact with the virally infected cell process. *h2*, Fluorescence intensity graph of IFN- γ (green) and LFA-1 (red) along the cell outline (white line, *g2*) demonstrating the highest levels of intensity of IFN- γ located centrally. *i2*, 3-D images were reconstructed along the interface (yellow line) and viewed en face (from the direction of the white arrow) to reveal centrally polarized distribution of IFN- γ (*j2*, green) and LFA-1 (*k2*, red). *l2*, Merged 3-D reconstructed images showing the central localization of IFN- γ . Scale bar (*f1*) = $10 \mu\text{m}$. *B* shows a schematic of the method to quantitate the diameter of the various constituents of the non-Kupfer type immunological synaptic contacts. The diameter of the synaptic interface (I) at non-Kupfer type immunological synaptic contacts was defined by the external limit of TCR distribution, the diameters of LFA-1 distribution and IFN- γ clusters were determined by their specific immunoreactivity. No statistical difference was found between the measurements. The results are based on the quantification of 13 non-Kupfer type synaptic contacts displaying polarized IFN- γ . *C* shows the average diameter of the synaptic interface (I) was $\sim 4.2 \mu\text{m}$, the average diameter of LFA-1 distribution was $\sim 4 \mu\text{m}$. The IFN- γ cluster displayed a smaller diameter ($2.6 \mu\text{m}$).

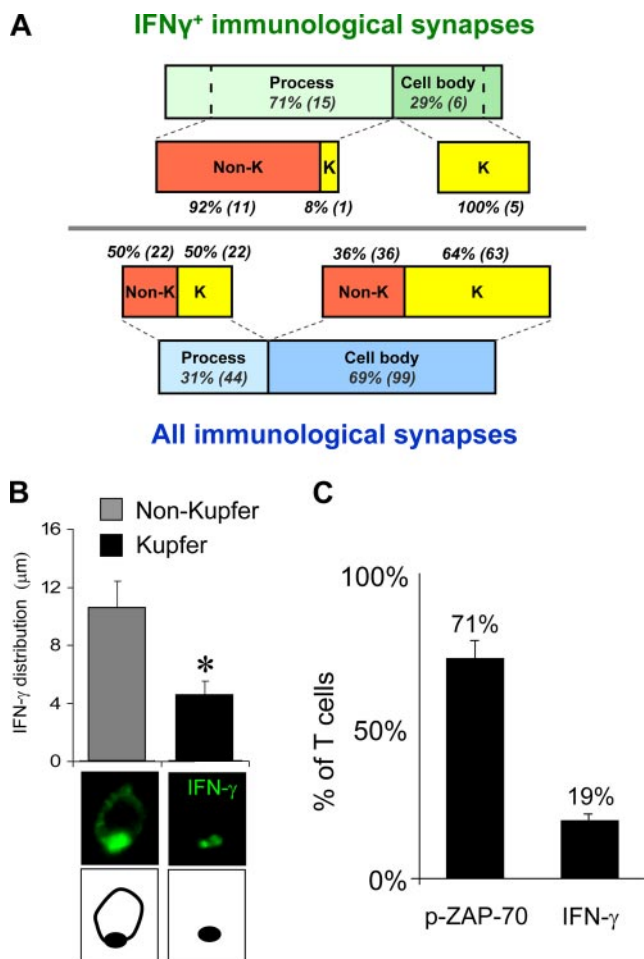


FIGURE 5. The majority of immunological synapses displaying clusters of IFN- γ are localized on the cell process and display a non-Kupfer-like phenotype. **A**, Quantification of the distribution of immunological synaptic contacts (i.e., Kupfer-type [K] or non-Kupfer type [non-K]) along cell processes or cell bodies of virally infected cells. The majority of immunological synaptic contacts displaying IFN- γ clusters are localized on the cell processes ($n = 15$, 71%); of those, most were non-Kupfer type contacts (92%). Of all synaptic contacts containing IFN- γ , four could not be assigned to either the Kupfer or non-Kupfer category; therefore, a total of 21 synaptic contacts containing IFN- γ were localized to either cell bodies or processes, although only 17 could be classified as Kupfer or non-Kupfer. Interestingly, the distribution of a large population of immunological synapses was different; i.e., the majority were localized to the cell body ($n = 99$, 69%); of these, most displayed Kupfer type morphology ($n = 63$, 64%). Immunological synaptic contacts localized on distal processes ($n = 44$, 31%) displayed an equal proportion of either Kupfer-type or non-Kupfer-type morphology. **B**, Detailed confocal analysis reveals that the area occupied by IFN- γ clusters (green) is significantly larger in non-Kupfer type synaptic contacts compared with Kupfer-type contacts (*, $p < 0.05$, Student's t test). **C**, Approximately 20% of all brain-infiltrating T cells expressed IFN- γ ; while 71% were immunoreactive for p-ZAP-70.

IFN- γ , a lower percentage than those containing phosphorylated-ZAP-70 (Fig. 5C).

Polarization of granzyme-B immunoreactivity toward infected astrocytes, and evidence of in vivo cytotoxicity of virally infected brain cells

We also studied the distribution of granzyme-B during the immune mediated clearance of infected astrocytes (Fig. 6A). As with IFN- γ , we could detect a polarized distribution of granzyme-B toward infected astrocytes (Fig. 6B). The polarized distribution of

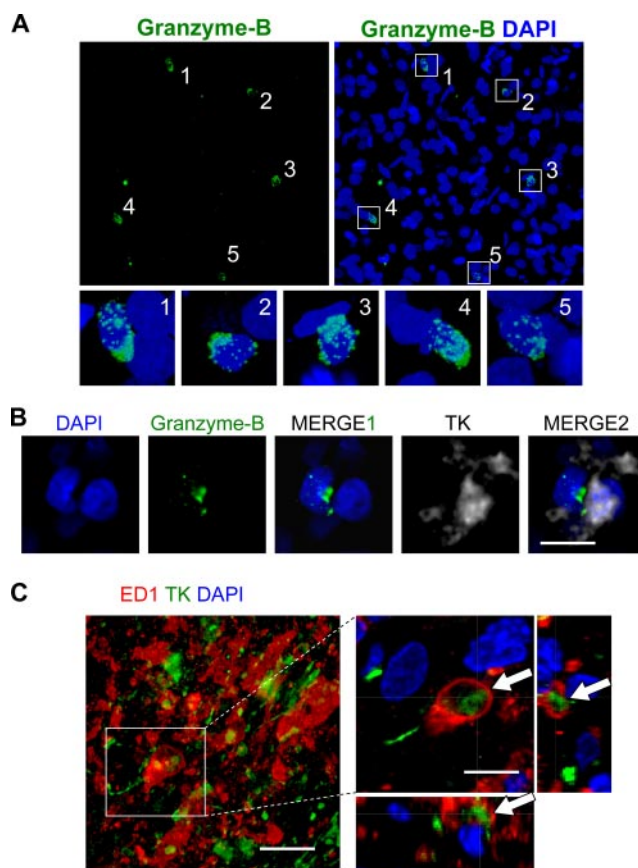


FIGURE 6. Polarization of granzyme-B, and macrophages/microglia engulf virally infected brain cell remnants. **A**, Top panels show confocal images of cells containing granzyme-B (green) in the striatum during the antiviral immune response; nuclei (DAPI, blue). Five cells shown at higher magnification, 1–5, all display a polarized distribution of granzyme-B (bottom panels). Granzyme-B immunoreactive cells were only found in the injected striatum of animals that had been immunized systemically against adenovirus. **B**, A granzyme-B immunoreactive cell (green) in close apposition with an infected brain cell (HSV1-TK, white) shows polarized clustering of granzyme-B toward the infected cell. Scale bar = 15 μ m. **C**, Confocal images show activated macrophages/microglia within the striatum (ED1; red) containing HSV1-TK-immunoreactive cellular debris (green). A higher magnification of the boxed area in the left panel is displayed on the right; this illustrates a macrophage/microglial cell that has engulfed HSV1-TK immunoreactive cellular debris. Lateral views indicate that the HSV1-TK immunoreactive debris appear to be located within the macrophage/microglial cell (arrows). Macrophages/microglia containing HSV1-TK immunoreactive debris were only found within the infected hemisphere of immunized animals. Scale bars, left, 20 μ m, right, 10 μ m.

granzyme-B is one known mechanism of T cell mediated cytotoxicity. That T cell killing of astrocytes in the CNS is ongoing, is suggested by the increase in the number of activated macrophages/microglia in the areas of brain inflammation during the clearance of virally infected astrocytes. Further, we could detect activated macrophages/microglia containing HSV1-TK, a protein exclusively expressed in infected astrocytes (Fig. 6C). Because activated macrophages/microglia containing HSV1-TK are never detected in the absence of immune infiltration, this suggests that macrophages have phagocytosed dead infected astrocytes.

Discussion

The detailed dynamics of the anti-adenoviral immune response in the brain were described by us earlier (1). In our model the peak

influx of CD8⁺ T cells into the brain occurs 14 days post immunization, while the peak influx of CD4⁺ T cells occurs at day 30. Furthermore, the vast majority of CD4⁺ T cells remain mostly within the perivascular compartment (1). All experiments conducted herein were done in animals 14 days post immunization; at this time point T cells infiltrating the striatum and establishing immunological synapses with infected astrocytes are CD8⁺ T cells. Further, we have also previously shown that infected astrocytes express MHC-I (1); however, the presence of MHC-II expression on astrocytes remains inconclusive.

Also, we have previously characterized in detail the brain cell types expressing HSV1-TK from our adenoviral vectors. More than 85% of cells expressing HSV1-TK were astrocytes while none contained the neuronal marker NeuN; additionally, we have been consistently unable to detect expression of HSV1-TK within microglia/macrophages (1). All previously described immunological synapses at day 14 postimmunization had been formed between CD8⁺ T cells and infected astrocytes. Taken together, published data support the assertion that the immunological synapses described herein are formed between antiviral CD8⁺ T cells and virally infected astrocytes.

In the present work we demonstrate that during the clearance of virally infected astrocytes from the brain effector molecules of CTLs, IFN- γ and granzyme-B, are polarized toward the immunological synaptic junction formed *in vivo*, between the antiviral T cells and the infected brain astrocytes (5, 9, 28–31). Importantly, we demonstrate that while IFN- γ polarization was detected within Kupfer-type immunological synapses, it can also be found within non-Kupfer type synaptic contacts that lack the typical organization of the c-SMAC and p-SMAC. This clearly indicates that the formation of a Kupfer-type immunological synapse is **not** necessary for the polarized targeting, and potential secretion, of effector cytokines and enzymes toward the immunological synaptic junction between the CTL and the target virally infected astrocytes *in vivo*.

We also established that the majority of immunological synapses formed by T cells are Kupfer-type junctions, and that these are mainly formed onto the cell bodies of target astrocytes. Synapses containing polarized IFN- γ clusters, however, formed mainly non-Kupfer type synapses, and most of these were established onto the astrocytes' processes. Whether non-Kupfer type junctions become Kupfer-type (or vice-versa), or whether the anatomical site of synapse formation is stochastic, remains to be determined by future live analysis of synapse formation in our model.

IFN- γ expression in immunological synapses was polarized, and this correlates with previous results obtained *in vitro* (6); *in vivo*, IFN- γ was polarized at the synaptic interface of both Kupfer-type, and non-Kupfer type synaptic junctions. In our *in vivo* model, granzyme-B was also found polarized to the synaptic contact interface confirming the potential directional secretion of effector molecules at immunological synapses *in vivo*. Other cytokines, such as TNF- α , have a different pattern of secretion *in vitro* (i.e., TNF- α is secreted outside of the synaptic interface) (6). Interestingly, the percentage of immunological synapses that contained IFN- γ clusters was lower than the percentage of immunological synapses that showed TCR activation (i.e., containing p-ZAP-70). This could either indicate that activation of different types of T cells utilize different effector molecules, or that in the brain TCR activation does not necessarily lead to production of effector molecules in all T cells. Alternatively, it could indicate that IFN- γ can only be detected over a short period. The detailed kinetics of activation, arming, and function of immunological synapses in the brain *in vivo*, will require the development of novel techniques to

monitor simultaneously the formation of different types of immunological synapses, and their concomitant activation of TCR signaling and effector molecule deployment.

We also determined that Kupfer-type synaptic junctions appear to be very stable structures and although the shape of the T cell can be very variable, this does not appear to affect significantly the structure and size of Kupfer-type junctions. Measurements of the IFN- γ clusters also demonstrated that IFN- γ clusters are smaller than the space left by the LFA-1 ring (p-SMAC), or space occupied by the TCR (c-SMAC). Our results are compatible with those obtained previously *in vitro* indicating the existence of a secretory domain within immunological synapses formed by CTL cells in the process of an antiviral brain immune response (5, 9).

Altogether, these results suggest that T cell activation, polarized and clustered deployment of effector molecules, and formation of immunological synapses occur in the brain *in vivo* during an antiviral immune response that clears infected astrocytes from the brain. Throughout, T cells become polarized toward the target cell, deploying effector molecules toward the synaptic interface, and finally secreting these toward the target Ag presenting cell. In conclusion, we found that during an antiviral brain immune response, full activation and effector function of CTLs *in vivo* does occur at non-Kupfer type immunological synapses, demonstrating that the classic Kupfer-type immunological synapse is not absolutely necessary for the potential polarized secretion of T cell effector molecules, and that various types of immunological synaptic structures underlie the function of antiviral CTLs in the brain *in vivo* during the clearance of infected cells.

A crucial aspect in the field of immunological synapses concerns the ultimate determination of the structure: function relationship of immunological synapses *in vivo*. It has been technically unfeasible to do so at this time due to physical limitations in microscopy and molecular methods available. In the future it will be important to develop appropriate tools to carefully correlate the temporal sequence of changes in immunological synaptic morphology (e.g., formation of p- and c-SMAC, and polarized distribution of effector molecules), with functional consequences of T cell-target cell interactions (e.g., TCR activation, effector cytokine secretion, target cell death etc.).

Acknowledgments

We thank Drs. Mark Davis and Yuri Sykulev for their careful and detailed review of our manuscript. We thank the support and academic leadership of Drs. S. Melmed and L. Fine.

Disclosures

We have no financial conflict of interest.

References

1. Barcia, C., C. E. Thomas, J. F. Curtin, G. D. King, K. Wawrowsky, M. Candolfi, W. D. Xiong, C. Liu, K. Kroeger, O. Boyer, et al. 2006. *In vivo* mature immunological synapses forming SMACs mediate clearance of virally infected astrocytes from the brain. *J. Exp. Med.* 203: 2095–2107.
2. Grakoui, A., S. K. Bromley, C. Sumen, M. M. Davis, A. S. Shaw, P. M. Allen, and M. L. Dustin. 1999. The immunological synapse: a molecular machine controlling T cell activation. *Science* 285: 221–227.
3. Monks, C. R., B. A. Freiberg, H. Kupfer, N. Sciaky, and A. Kupfer. 1998. Three-dimensional segregation of supramolecular activation clusters in T cells. *Nature* 395: 82–86.
4. Kupfer, A., G. Dennert, and S. J. Singer. 1983. Polarization of the Golgi apparatus and the microtubule-organizing center within cloned natural killer cells bound to their targets. *Proc. Natl. Acad. Sci. USA* 80: 7224–7228.
5. Stinchcombe, J. C., E. Majorovits, G. Bossi, S. Fuller, and G. M. Griffiths. 2006. Centrosome polarization delivers secretory granules to the immunological synapse. *Nature* 443: 462–465.
6. Huse, M., B. F. Lillemeier, M. S. Kuhns, D. S. Chen, and M. M. Davis. 2006. T cells use two directionally distinct pathways for cytokine secretion. *Nat. Immunol.* 7: 247–255.
7. Dustin, M. L. 2005. A dynamic view of the immunological synapse. *Semin. Immunol.* 17: 400–410.

8. Irvine, D. J. 2003. Function-specific variations in the immunological synapses formed by cytotoxic T cells. *Proc. Natl. Acad. Sci. USA* 100: 13739–13740.
9. Stinchcombe, J. C., G. Bossi, S. Booth, and G. M. Griffiths. 2001. The immunological synapse of CTL contains a secretory domain and membrane bridges. *Immunity* 15: 751–761.
10. Huppa, J. B., and M. M. Davis. 2003. T-cell-antigen recognition and the immunological synapse. *Nat. Rev. Immunol.* 3: 973–983.
11. Brossard, C., V. Feuillet, A. Schmitt, C. Randriamampita, M. Romao, G. Raposo, and A. Trautmann. 2005. Multifocal structure of the T cell-dendritic cell synapse. *Eur. J. Immunol.* 35: 1741–1753.
12. Trautmann, A., and S. Valitutti. 2003. The diversity of immunological synapses. *Curr. Opin. Immunol.* 15: 249–254.
13. Revy, P., M. Sospedra, B. Barbour, and A. Trautmann. 2001. Functional Ag-independent synapses formed between T cells and dendritic cells. *Nat. Immunol.* 2: 925–931.
14. Davis, M. M., M. Krogsgaard, M. Huse, J. Huppa, B. F. Lillemeier, and Q. J. Li. 2007. T cells as a self-referential, sensory organ. *Annu. Rev. Immunol.* 25: 681–695.
15. Blanchard, N., V. Di Bartolo, and C. Hivroz. 2002. In the immune synapse, ZAP-70 controls T cell polarization and recruitment of signaling proteins but not formation of the synaptic pattern. *Immunity* 17: 389–399.
16. Holdorf, A. D., K. H. Lee, W. R. Burack, P. M. Allen, and A. S. Shaw. 2002. Regulation of Lck activity by CD4 and CD28 in the immunological synapse. *Nat. Immunol.* 3: 259–264.
17. Lee, K. H., A. D. Holdorf, M. L. Dustin, A. C. Chan, P. M. Allen, and A. S. Shaw. 2002. T cell receptor signaling precedes immunological synapse formation. *Science* 295: 1539–1542.
18. Yachi, P. P., J. Ampudia, N. R. Gascoigne, and T. Zal. 2005. Nonstimulatory peptides contribute to antigen-induced CD8-T cell receptor interaction at the immunological synapse. *Nat. Immunol.* 6: 785–792.
19. Yokosuka, T., K. Sakata-Sogawa, W. Kobayashi, M. Hiroshima, A. Hashimoto-Tane, M. Tokunaga, M. L. Dustin, and T. Saito. 2005. Newly generated T cell receptor microclusters initiate and sustain T cell activation by recruitment of Zap70 and SLP-76. *Nat. Immunol.* 6: 1253–1262.
20. O'Keefe, J. P., and T. F. Gajewski. 2005. Cutting edge: cytotoxic granule polarization and cytolysis can occur without central supramolecular activation cluster formation in CD8⁺ effector T cells. *J. Immunol.* 175: 5581–5585.
21. Lettau, M., J. Qian, A. Linkermann, M. Latreille, L. Larose, D. Kabelitz, and O. Janssen. 2006. The adaptor protein Nck interacts with Fas ligand: guiding the death factor to the cytotoxic immunological synapse. *Proc. Natl. Acad. Sci. USA* 103: 5911–5916.
22. Shi, L., D. Keefe, E. Durand, H. Feng, D. Zhang, and J. Lieberman. 2005. Granzyme B binds to target cells mostly by charge and must be added at the same time as perforin to trigger apoptosis. *J. Immunol.* 174: 5456–5461.
23. Faroudi, M., R. Zaru, P. Paulet, S. Muller, and S. Valitutti. 2003. Cutting edge: T lymphocyte activation by repeated immunological synapse formation and intermittent signaling. *J. Immunol.* 171: 1128–1132.
24. Purbhoo, M. A., D. J. Irvine, J. B. Huppa, and M. M. Davis. 2004. T cell killing does not require the formation of a stable mature immunological synapse. *Nat. Immunol.* 5: 524–530.
25. Dewey, R. A., G. Morrissey, C. M. Cowsill, D. Stone, F. Bolognani, N. J. Dodd, T. D. Southgate, D. Klatzmann, H. Lassmann, M. G. Castro, and P. R. Lowenstein. 1999. Chronic brain inflammation and persistent herpes simplex virus 1 thymidine kinase expression in survivors of syngeneic glioma treated by adenovirus-mediated gene therapy: implications for clinical trials. *Nat. Med.* 5: 1256–1263.
26. Thomas, C. E., G. Schiedner, S. Kochanek, M. G. Castro, and P. R. Lowenstein. 2000. Peripheral infection with adenovirus causes unexpected long-term brain inflammation in animals injected intracranially with first-generation, but not with high-capacity, adenovirus vectors: toward realistic long-term neurological gene therapy for chronic diseases. *Proc. Natl. Acad. Sci. USA* 97: 7482–7487.
27. Barcia, C., C. Gerdes, W. Xiong, C. E. Thomas, C. Liu, K. M. Kroeger, M. G. Castro, and P. R. Lowenstein. 2006. Immunological thresholds in neurological gene therapy: highly efficient elimination of transduced cells may be related to the specific formation of immunological synapses between T cells and virus-infected brain cells. *Neuron Glia Biol.* 2: 309–327.
28. Gomez, T. S., K. Kumar, R. B. Medeiros, Y. Shimizu, P. J. Leibson, and D. D. Billadeau. 2007. Formins regulate the actin-related protein 2/3 complex-independent polarization of the centrosome to the immunological synapse. *Immunity* 26: 177–190.
29. Billadeau, D. D., J. C. Nolz, and T. S. Gomez. 2007. Regulation of T-cell activation by the cytoskeleton. *Nat. Rev. Immunol.* 7: 131–143.
30. Rey, M., F. Sanchez-Madrid, and A. Valenzuela-Fernandez. 2007. The role of actomyosin and the microtubular network in both the immunological synapse and T cell activation. *Front. Biosci.* 12: 437–447.
31. Combs, J., S. J. Kim, S. Tan, L. A. Ligon, E. L. Holzbaur, J. Kuhn, and M. Poenie. 2006. Recruitment of dynein in the Jurkat immunological synapse. *Proc. Natl. Acad. Sci. USA* 103: 14883–14888.
32. Anikeeva, N., K. Somersalo, T. N. Sims, V. K. Thomas, M. L. Dustin, and Y. Sykulev. 2005. Distinct role of lymphocyte function-associated antigen-1 in mediating effective cytolytic activity by cytotoxic T lymphocytes. *Proc. Natl. Acad. Sci. USA* 102: 6437–6442.